

Seasonal and annual variation of heat balance in the western Tibet.

Shigenori Haginoya
Meteorological Research Institute
1-1, Nagamine, Tsukuba, Ibaraki 305-0052, JAPAN
shaginoy@mri-jma.go.jp

1. Introduction

Tibetan Plateau is one of the most important areas to affect the Asian Monsoon caused through Air-Sea-Land interactions. It has wide area, 1000km from south to north and 2000km from east to west, is located in the middle latitude and penetrates the middle of troposphere. Therefore it has large effect on heating the middle of troposphere directly. It is very important to clarify the heat and water balance between the ground surface and the atmosphere over Tibetan Plateau.

Tibetan Plateau consists of two main climate regions. One is eastern wet region and the other is western dry region. The previous study pointed out that the remarkable differences are found in the ratio of sensible heat flux to latent heat flux between the two regions (Zhang et al., 1988). Sensible heat flux is dominantly in the western Tibet. However this observation is from May to August, therefore there is no reliable data to estimate the heat balance throughout the year. Especially, western part of Tibetan Plateau has few observatories compared with eastern Tibet.

AWS observation has been started in the western Tibet since 1997. The observation data throughout the year were obtained and the heat balance of winter became clear (Haginoya, 2000). We have been applying the Bowen ratio method and calculating the long-term heat balance in the Tibetan Plateau. The Bowen ratio method has the following merits: (1) it can cancel systematic errors in the wind velocity. (2) it uses net radiation flux and ground heat flux. The precision of sensible heat flux and latent heat flux correspond to those of net radiation flux and ground heat flux. If the precision of net radiation flux and ground heat flux measurement are good, then those of sensible heat flux and latent heat flux are also good.

Because the western Tibet is the area where all the precipitation evaporates (Xu and Haginoya, 2001), annual variation of evaporation strongly depends on precipitation. Precipitation changes Bowen ratio and has effect on sensible heat flux which heats the atmosphere directly.

As explained above, until now, seasonal variation of heat balance was already obtained. Next step is to answer the question; "How large is the annual variation?" The research of this field is done by the model calculation which was used routine data (Xu and Haginoya, 2001). However, there is no result which was applied Bowen ratio method.

This study aims to collect the basic meteorological data including temperature and humidity differences between two levels, radiation

Table 1 Summary of AWS sites

Site name	<i>Gaize</i>	<i>Shiquanhe</i>
Latitude	32° 18'N	32° 30'N
Longitude	84° 03'E	80° 05'E
Altitude(m)	4,420	4,279
Around the topography	flat	flat, surrounded mountain
Conditions around the site	rural	rural town
Ground surface conditions	bare soil, few grasses	bare soil, no grass

and soil moisture, and to estimate heat budgets in the western part of Tibetan Plateau for several years then to clear the seasonal and annual variation of the western Tibet.

2. Observation

2.1 Observation field

Two sets of Automatic Weather Station (AWS) have been installed in the western Tibet and continued observation since the end of September in 1997. AWS were installed inside the routine meteorological observatory for easy maintenance and safety. Table 1 shows characteristics of the observation sites. One of the sites is Gaize that is located at the middle of western Plateau. The other site is Shiquanhe that is located in the western edge of Tibetan Plateau. The ground surface conditions of both sites are bare soil, few grasses and no tree.

2.2 Automatic Weather Station (AWS)

The present AWS has the function to measure the meteorological elements automatically and to record the data necessary for heat budget analysis on the ground surface. The measured elements are the following items; wind speed (4, 2 and 1m high, three levels), temperature and humidity (3.6, 2 and 1m high, three levels from Sep. 1997 to Sep. 1999, 3.6 and 0.5m high, two levels since Sep. 1999), the four components of radiation, the ground surface radiation temperature, soil moisture (from 0 to 15cm and from 15 to 30cm in depth, two layers from Sep. 1997 to Sep. 1999, from 0 to 6cm, 6 to 16cm and 16 to 26cm in depth, three layers since Sep. 1999), precipitation, surface pressure, wind direction, soil heat flux (2.5cm and 7.5cm in depth, two levels) and soil temperature (0, 5, 10, 20, 40 and 80cm in depth, 6 levels). All the sensors are controlled by CR10X (Campbell Scientific, Inc.). Recording interval is one hour. Wind direction is 10 minutes average before

every hour. Wind speed is scalar average. Radiation data are integrated every 10 seconds sampling. Other data (temperature, relative humidity, pressure and soil moisture) are instantaneous value. AWS can store data for the period of more than one year at one hour interval. AWS works with solar cell and storage battery.

3. Data

The AWS data were collected until September 2000. Figure 1 and 2 show the time series of some elements at Shiquanhe. Detail explanations of them are referred to the following sub-sections.

3.1 Radiation

Radiation is the largest elements of heat balance equation. Each sensor was calibrated before installation and compared the spare sensor every year. Because the observation was carried out automatically, the collected data should be checked to increase the reliability.

Global solar radiation ($S \downarrow$) in clear day can be checked. The thin solid lines in the Figure 1 show the calculated global solar radiation in clear air conditions. Parameter (b) is Angstrom's turbidity coefficient (Kondo and Miura, 1983). The top line shows $b=0$ and the lowest one 0.08. The marks indicate the daily average of observation data. The maximum value which is considered the clear air conditions reaches the thin line, so we conclude the global solar radiation data is consistent.

Downward long wave radiation ($L \downarrow$) was checked by empirical formula (Kondo & Xu, 1997). Figure 2 shows the calculated downward long wave radiation in clear air condition (thick line) and cloudy condition (thin line). The marks (observation) are scattered around them. It is found that the large global solar radiation data in Fig. 1 correspond to small downward long wave radiation data in Fig. 2.

Upward long wave radiation ($L \uparrow$) was checked by the following formula (1).

$$L_{cal} \uparrow = \epsilon_s T_s^4 + (1 - \epsilon) L \downarrow \quad (1)$$

Where T_s is the ground surface temperature, ϵ is emissivity. $L \uparrow$ is compared with $L_{cal} \uparrow$.

Net radiation Rn is calculated by equation (2);

$$Rn = S \downarrow - S \uparrow + L \downarrow - L \uparrow \quad (2)$$

where $S \uparrow$ reflective solar radiation. Net radiation is positive even in winter season with no snow. This is due to large global solar radiation. On the other hand, once it snowed, net radiation became negative. This is due to increase of surface albedo.

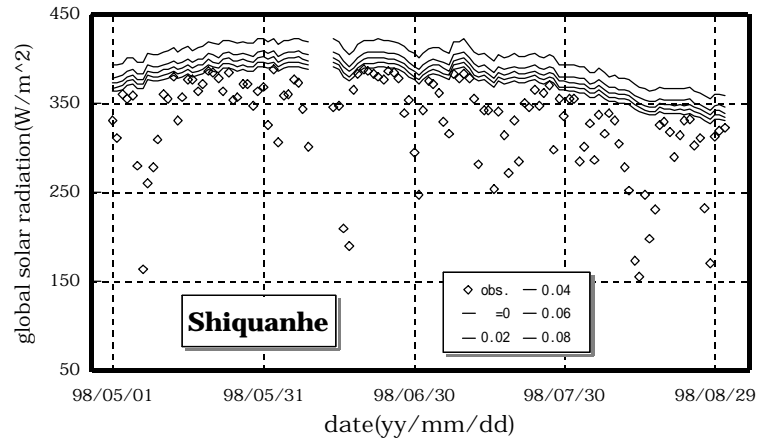


Figure 1 Global solar radiation, observation (mark) and calculation (line).

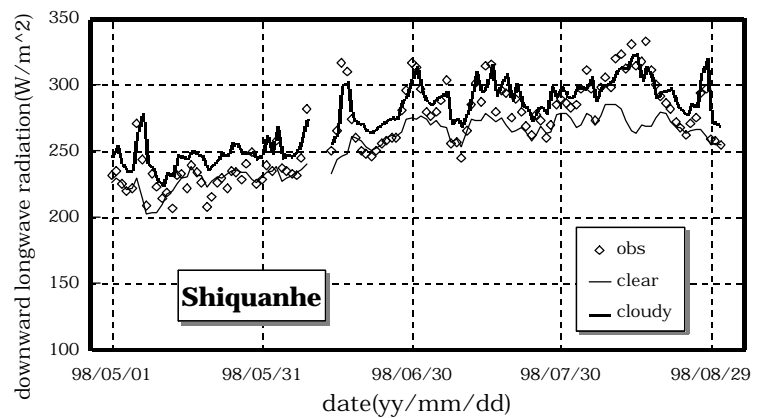


Figure 2 Downward long wave radiation, observation (mark) and calculation (line).

3.2 Albedo and soil moisture

The albedo ($= S \uparrow / S \downarrow$) gives the ground surface conditions not only covering such as snow, grass or bare soil but also soil moisture. Figure 3 shows the relation between albedo and surface soil moisture averaged from 0 to 6cm depth. Albedo decreases with increase of soil moisture from May to August.

3.3 Soil heat flux

Heat capacity of soil is estimated the equation (3).

$$c_g \mathbf{r}_g = \frac{G_{2.5} - G_{7.5}}{\frac{\partial}{\partial t} \int_{2.5}^{7.5} T_g dz} \quad (3)$$

Then soil heat flux at ground surface (G_0) was estimated equation (4).

$$G_0 = \int_0^{2.5} c_g \mathbf{r}_g \frac{\partial T_g}{\partial t} dz + G_{2.5} \quad (4)$$

Where $G_{2.5}$ and $T_{2.5}$ mean soil heat flux and soil temperature at 2.5cm in depth, respectively.

Average value of $c_g \mathbf{r}_g$ is 2.1×10^6 (J/K/m³) which is between dry and wet value of clay soil or sand soil. Soil heat flux changes the direction during February

and August. Its amplitude of annual variation is about 10W/m^2 .

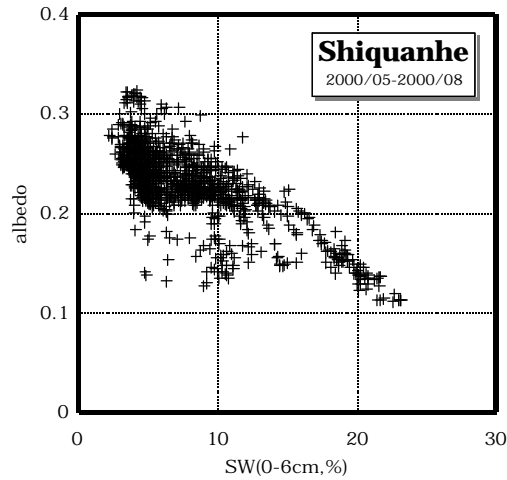


Figure 3 The relation between albedo and surface soil moisture from 0 to 6cm depth.

4. Heat balance analysis

Equation (5) expresses the surface heat balance.

$$Rn = H + IE + G \quad (5)$$

The present AWS can measure the four components of radiation flux (Rn) and soil heat flux (G) directly. Sensible heat flux (H) and latent heat flux (IE) are estimated by the Bowen ratio method. The Bowen ratio (B) is defined by the ratio of sensible heat flux to latent heat flux as equation (6).

$$B = \frac{H}{IE} \quad (6)$$

$$H = C_p r K_H \frac{\partial T}{\partial z} \quad (7)$$

$$IE = i r K_E \frac{\partial q}{\partial z} \quad (8)$$

where, T : air temperature, q : specific humidity, z : height, C_p : specific heat at constant pressure, r : air density, i : latent heat of vaporization, K_H : eddy diffusivity of heat, and K_E : eddy diffusivity of water vapor.

The Bowen ratio is equal to the ratio of temperature difference to specific humidity difference

with the assumption of $K_H=K_E$.

$$B = \frac{C_p K_H \frac{\partial T}{\partial z}}{i K_E \frac{\partial q}{\partial z}} \cong \frac{C_p T_1 - T_2}{i q_1 - q_2} \quad (9)$$

Suffixes 1 and 2 express the level.

The key point of the Bowen ratio method is how to measure the temperature differences and specific humidity differences with the necessary accuracy. The remodeled AWS can measure temperature and humidity differences within 0.05C and 0.5% , respectively. The error of Bowen ratio method was shown below 10W/m^2 (Haginoya, 2000). Once we obtain the Bowen ratio, we can estimate the sensible heat flux and latent heat flux from the equation (10) and (11).

$$IE = \frac{Rn - G}{1 + B} \quad (10)$$

$$H = B \frac{Rn - G}{1 + B} \quad (11)$$

Figure 4 shows the monthly variation of heat balance and precipitation from October in 1997 to July in 2000. The sign of H , IE , and G are defined positive when the flux goes out of the surface. From the heat balance equation (5), $Rn-G=H+IE$. $Rn-G$ has a minimum value in December and maximum value in June to August. Most part of ($Rn-G$) balances with H . IE is small value in dry season and becomes large in rainy season. The magnitude of net radiation or latent heat flux strongly depends on the existence of precipitation. Net radiation in August 1999 and July 2000 are larger than the same month of other year. This will be discussed the next section. Table 2 shows the annual average of heat fluxes in 1998 and 1999. Total rainfall in 1998 is about half in 1999. Variation of $Rn-G$ is small. Bowen ratio corresponds to the difference of rainfall.

Table 2 Annual value of heat balance elements at Shiquanhe. * is converted into energy flux.

Year	1998	1999
$Rn-G(\text{W/m}^2)$	59.6	60.5
$H(\text{W/m}^2)$	52.4	50.3
$IE(\text{W/m}^2)$	7.1	10.2
Bowen ratio	7.3	4.9
Rainfall(mm)	47.1	111.6
Rainfall(W/m^2)*	3.7	8.7

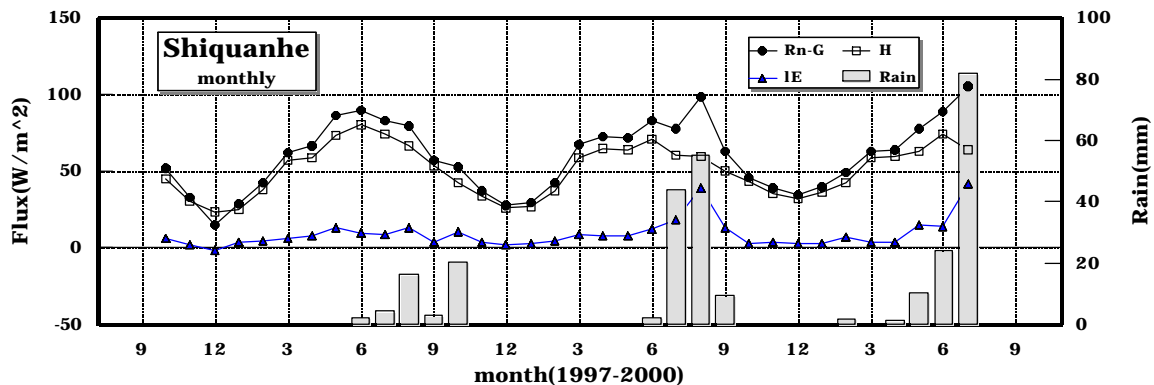


Figure 4 Monthly heat balance and precipitation.

5. Discussion

Latent heat flux strongly depends on the existence of precipitation because the large amount of rainfall increases the soil moisture then the evaporation from the ground surface becomes active.

On the other hand, radiation flux also depends on the existence of precipitation. The large amount of rainfall increases the evaporation from the ground surface then the evaporation suppresses the rise of ground surface temperature. This means to decrease upward long wave radiation $L \uparrow$. Another effect of precipitation is to increase soil moisture then it decreases albedo (see Fig. 3). Therefore reflective solar radiation $S \uparrow$ becomes small. The other cause is to increase downward long wave radiation $L \downarrow$ and to decrease global solar radiation $S \downarrow$ due to cloudy weather. These three effects make net radiation become larger except for $S \downarrow$. Figure 5 shows the total effects of precipitation increase R_n .

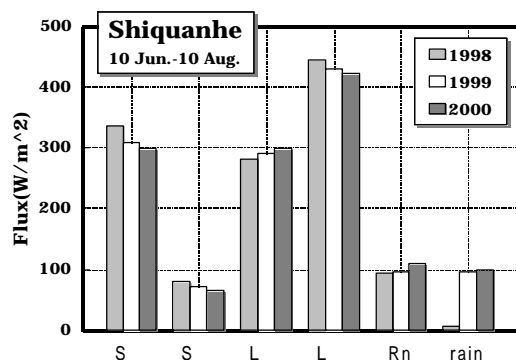


Figure 5 Comparison of radiation fluxes averaged from 10 Jun. to 10 Aug.

6. Acknowledgment

The authors express their gratitude to Mr. T. Onogaya of Agematsu Seiki Co. Ltd. for his support of field work. The authors express their thanks to Mr. Qun Jue and his staffs of Tibetan Meteorological Bureau for their kindly help in Tibet. The authors also express their thanks to the local staffs of meteorological observatory at Gaize and Shiquanhe for their routine maintenance work.

This study was supported by Science and Technology Agency (until 1998JFY) and Frontier Observation System for Global Change (after 1999JFY). The field observation is carried out in cooperation with China Meteorological Administration (CMA).

7. References

- Haginoya, S. and H. Naoe, 2000: Surface Heat Balance Observation in the Western Tibet. Preprints 15th Conference on Hydrology, 9-14 Jan., 2000, LongBeach, California, 301-304.
- Haginoya, S., 2000: Study on Surface Heat Balance in the Tibetan Plateau -Precision of Bowen Ratio

Method-. Preprints Volume The Second Session of International Workshop on TIPEX-GAME/TIBET, Kunming, China 20-22 Jul., 2000, 19-21.

- Kondo, J. and A. Miura, 1983: Empirical formula of the solar radiation at the ground level and a simple method to examine an inaccurate pyranometer. *Tenki*, **30**, 284-290.
- Kondo, J. and J. Xu, 1997: Seasonal variations in the heat and water balances for nonvegetated surfaces. *J. Appl. Meteor.*, **36**, 1676-1695.
- Xu, J. and S. Haginoya, 2001: An estimation of Heat and Water Balances in the Tibetan Plateau. *J. Met Soc. Japan*, in press.
- Zhang, J., B. Zhu, et. al, 1988: Advances in the Qinghai-Xizang Plateau Meteorology. The Qinghai-Xizang plateau meteorological experiment (1979) and research. pp.268.